Wideband Propagation Measurements for Wireless Indoor Communication

Peter B. Papazian and Robert J. Achatz
U.S. Department of Commerce
National Telecommunications and Information Administration
Institute for Telecommunication Sciences
325 Broadway
Boulder, Colorado 80303 USA
Telephone: (303) 497-3498

Introduction

Because of the importance of wireless local area networks to the U.S. economy, the Institute for Telecommunication Sciences (ITS) has implemented a wideband measurement system to aid in standards development. This report presents a preliminary view of indoor channel propagation measurements and the metrology used in collection and analysis of indoor multipath interference data. At present the development of acquisition and analysis metrology is not complete. It is hoped that cooperative efforts with industry can be used to guide further developments.

Measurement System

The ITS wideband probe is used to measure indoor channel propagation characteristics. The system, which has a bandwidth of 1 GHz, has previously been used for outdoor millimeter wave propagation experiments in urban and vegetated settings as described in [1], [2], and [3]. For indoor measurements, the probe was modified to transmit a 1.5 GHz carrier with BPSK modulation. The modulation code is a 127 bit pseudo random sequence with bit rate adjustable between 100 and 500 MB/s. Wideband, vertically polarized, omnidirectional antennas were used at the transmitter and receiver. The system measures cophase and quadphase channel response using a sliding correlator. By adjusting the sliding correlator's clock offset frequency, channel responses were measured every 100 ms and stored on a digital analog tape recorded (DAT) for later computer processing. A block diagram of the system is shown in Figures 1 and 2. The

detector sensitivity is limited by its correlation noise level. The detector's dynamic range is determined by the 127 bit PN word length and is 42 dB. Dynamic range of the system is determined by the DAT, which employed a 16 bit A/D converter with a range of 90 dB. By using variable gain video amplifiers in the DAT, the signal voltage was maintained above the noise floor at all measurement sites.

Data Processing

The DAT medium allows complete storage of cophase and quadphase channel responses for 2 hours of continuous measurements. In our tests, the receiver was stationary while the transmitter was moved on a cart at a constant speed along a predetermined path. Data are stored in records that contained the two channels of digital data representing n discrete channel responses recorded for a particular profile. A DSP card is used to interface the DAT to a PC, which enables data transfer for processing and statistical analysis. Although impulses were collected every 100 ms, Doppler spread and coherence time were not included in the processing. This may be added in the future. However, we did include the ability to spatially average the data, which would minimize large variations in delay spread from individual scatterers.

The first step in processing is to separate the n distinct channel responses recorded on a particular profile. To do this an autocorrelation is performed on the data to accurately determine the impulse repetition rate. Once this is accomplished, the peak of the first response (minus sufficient samples to account for the pulse rise time) is located to determine a beginning point of the record. Then the repetition rate is used to identify each succeeding response. Let $CO_i(\tau),(i=1,2..n)$ and $Quad_i(\tau),(i=1,2..n)$ be the n distinct cophase and quadphase voltage time sequences for each channel of a data profile. The power-delay profile (PDP), $P_i(\tau)$, is the channel impulse function squared, $I_i(\tau)^2$. For the ith record in a data profile, this is

$$P_i(\tau) = CO_i(\tau)^2 + Quad_i(\tau)^2$$

$$(1)$$

The PDP can also be averaged spatially by computing a running average of n adjacent impulse responses as the transmitter cart is moved, equation (2). The power delay is then normalized by total received power to obtain the averaged probability density function of excess delay, equation (3) [4, 5].

$$I_i^n(\tau)^2 = \frac{1}{n} \sum_{\alpha=i}^{i+n-1} I_\alpha(\tau)^2 (i=1,2.....j)$$

(2)

$$p_i^n(\tau)^2 = \frac{I_i^n(\tau)^2}{\int_0^\infty I_i^n(\tau)^2 d(\tau)}$$

(3)

The mean delay, $T0_i^n$, is then calculated using the statistical definition of first moment, equation (4).

$$T0_i^n = \int_0^\infty \tau p_i^n(\tau) d(\tau)$$

(4)

$$Td_i^n = \left[\int_0^\infty (\tau - T0_i^n)^2 p_i^n(\tau) d(\tau) \right]^{1/2}$$

(5)

The delay spread Td_i^n is defined as the square root of the variance, which is also the square root of the second central moment, equation (5). This integral is performed as a summation with maximum integration time equal to the sum of the word lengths of the averaged impulses or up to the time for any individual impulse when the signal decays to a predefined threshold level.

The signal level attenuation versus distance is tracked using peak power and energy per impulse. These quantities are normalized to 0 dB with the transmitter and receiver separated by 3 m. Peak power is the maximum of the PDP for each impulse response. Energy is the integral of the PDP equation (6). This is also the average cw power over the system bandwidth.

$$P_{i_{Total}}^n = \int_0^\infty P_i^n(\tau)d(\tau)$$

(6)

The correlation function [6] is computed using equation (7).

$$R(\Delta f) = F\left[p_i^n(\tau)\right]$$

(7)

The correlation bandwidth is then defined as the bandwidth at which the correlation drops by 50 percent.

Calibration

System calibration and delay spread processing algorithms were checked using two coaxial transmission lines to simulate a multipath signal in the laboratory. The calibration setup is shown in Figure 3. The delta time for signal arrival was calculated using cable manufacturer specifications. The attenuation of a 1.5 GHz cw signal was also measured. These results are listed in Table 1. Figure 4 shows the measurement results for one nonaveraged impulse response from a 10 s calibration test. Table 2 lists the measurement results verses the known characteristics of the unequal delay lines. Delay measurements for a random impulse were found to be accurate to about 5 percent and amplitude measurements agreed to about 7 percent.

Table 1. Delay Line Characteristics at 1.5 GHz

Cable #	V_p(m/s)	L(m)	T_d(ns)	A(dBm)
1(FWG)	2.40E+8	15.5	64.6	-5.67
2(RG55)	1.73E+8	1.5	8.67	-2.17

Table 2. Calibration Results for Known Delay Δt and Peak Signal Attenuation ΔA
Measured at 100M B/s and 500 MB/s

	Calculated	Measured 100, 500 MB/s	Percent Error 100, 500 MB/s
Δt(ns)	55.9	59, 58	5.5, 3.7
ΔA	0.45	0.417, 0.483	7.3, 7.3

A minimum delay spread measurement was also made. To do this a delay spread profile for a direct signal with no multipath was recorded for 10 s. The theoretical minimum delay spread for the system under these conditions was calculated for a triangular pulse 127 bits high with a base 2 bits wide. A threshold detection level of 20 dB was then used to perform the integration required in equation (5). Results from this test are given in Table 3.

Table 3. Measured Versus Calculated Minimum Delay Spreads for Direct Signal at 100 and 500 MB/s Using a 20 dB Threshold

	Calculated (ns)	*Measured* (ns)
T_{d100}	4.2	3.6
T_{d500}	0.8	1.1

Measurements

Delay spread measurements were made at three locations. Site #1 was a long hallway with cinder block walls at the Department of Commerce Boulder Laboratories. The hallway was flanked by offices on one side and laboratories on the other. Site #2 was the Commerce auditorium, also located at the Boulder Laboratories. This room is wood, paneled with metal seats, and a raised stage area. Site #3 was an open floor plan office with soft partitions at the US West Research Facility in Boulder, CO. Floor plans, transmitter, receiver, and data profile locations are shown in Figures 5, 6, and 7. In all cases the transmitter was moved on a cart along the profiles with a fixed receiver location. The receiver was positioned at a height of 2.1 m (7 ft). The transmitter height was 1.6 m (5.3 ft). This gave a clear line of sight (LOS) between the transmit and receive antennas in the hallway and the auditorium. In the soft partitioned office, all profiles except #1 and #2 were obstructed line of sight (OLOS). This obstruction was due to the soft partitions, which were 6 ft high and randomly spaced office furniture (see Figure 6).

Delay spreads were calculated from the received PDP using no averaging and a 20 dB threshold. Signal levels below threshold (20 dB below the peak signal) on a PDP are set to zero. This must be done so delay spread is not a function of integration time.

Because significant delays were encountered at the US West office on OLOS profiles, the 100 MB/s data were selected for reporting. This choice was made by monitoring the tail of each PDP. The ratio of the average value of the tail of the PDP and the peak signal of each PDP should be at least 20 dB. An example of this calculation is in Figure 8 and is labeled PDP Amplitude Ratio. The delay profile and PDP's associated with the minimum and maximum delay spreads for US West profile 4 are also shown in Figures 8. The correlation function for the maximum-minimum impulses from Figure 8 are shown in Figure 9. As can be seen, the FFT's (correlation function) of PDP's with larger delays decay more rapidly to the 3 dB points and have a smaller correlation bandwidth (BW). However, it can be seen by inspection of the max and min delay spreads and the corresponding 3 dB points of the correlation function that delay spread and correlation BW do not have a precisely inverse relationship in our calculations.

For comparison of these results with calibration data, the 3 dB points for direct signals with no delay spread are given in Table 4.

Table 4. Measured System Bit Rate Versus 3 dB Point of Correlation Function for a Direct Signal

Bit Rate (MB/s)	100	200	500
3 dB Point(MHz)	112	225	450

When making estimates of the correlation BW, the 3 dB points from Table 4 can be considered as upper limits for channel BW measurements. Correlation BW's approaching these numbers are really underestimates for the channel. To correct this, the system transfer function can be deconvolved in the processing. This would extend the usable correlation BW measurement ability of the system. This has not been done as yet but can be if the upper limits are considered important.

Delay spread, correlation BW, and attenuation versus position graphs have been compiled for all data profiles. These graphs display the calculated results for each PDP at 100 ms intervals again using a 20 dB threshold and no spatial averaging. The time sequence was then converted to distance by assuming a constant cart speed.

Figures 10, 11, and 12 are comparisons of delay spread profiles and correlation BW. Figure 10 shows the two LOS profiles at the US WEST office. Figure 11 displays the OLOS profiles from US WEST, and Figure 12 shows the LOS profiles measured at the Department of Commerce (DOC) sites. The somewhat inverse relationship between delay spread and CBW can be seen on all plots. In general, the delay spread magnitudes are dominated by the geometry of the measurement site. For LOS paths delay spread decreases slightly with increasing distance in the narrow DOC hallway (Figure 13) and has smaller delay spreads than the LOS measurements in the square plan auditorium (Figure 13). LOS paths in the US WEST office experience larger delay spreads up to 70 ns caused by possible multipath through windows and scattering off partitions.

OLOS paths at US WEST (Figure 11) exhibit the largest delays, which increase somewhat linearly with distance. Here we see maximum delay spreads around 200 ns on profiles 2, 3, 4, 5, 7, and 8.

Cumulative distributions and histograms of delay spread were compiled and are shown in Figures 14, 15, and 16. Median values of delay spread are 8.5, 24, and 65 ns for the hallway auditorium and soft partitioned office respectively.

Position data also were used to convert attenuation versus profile position to attenuation versus log euclidean distance [7] from the transmitter. Scatter plots were made for each profile, and the average slope was determined using a linear regression algorithm. Results are given in Figures 16, 17, and 18, and the average power law coefficients are summarized in Table 5.

Table 5 - Power Law Coefficients and Averages for LOS and OLOS Paths

Location	Type/#	Power Law Coefficients
DOC Hallway	LOS	1.41
DOC Auditorium	LOS	.898
US WEST Office	LOS/1	1.69
	LOS/6	.929
	OLSO/2	2.58
	OLSO/3	3.51
	OLSO/4	4.74
	OLSO/5	7.49
	OLOS/7	3.37
	OLOS/8	7.75
Average	LOS	1.23
	OLSO	4.91

An inspection of these coefficients shows an average below free space attenuation (coefficient 2) for indoor LOS paths. However, the attenuation coefficients for OLOS paths vary between 2.58 and 7.75. This would seem a large range, but is explained by the number of partitions blocking line of site on each path. It can be seen from Figure 6 that path 2 has the fewest partitions separating the transmitter and receiver and the smallest attenuation coefficient for the

OLOS paths. The coefficient then increases in a somewhat predictable pattern on paths 7, 3, 4, 5, and 8.

REFERENCES

[1]   E. J. Violette, R. H. Espeland, K. C. Allen, "A diagnostic probe to investigate propagation at millimeter wave lengths," NTIA Report 83-128, August 1983, (NTIS Order No. PB 84-104223).

[2]   E. J. Violette, K. C. Allen, et al., "Millimeter-wave urban and suburban propagation measurements using narrow and wide bandwidth channel probes," NTIA Report 85-184, 1985 (NTIS Order No. PB 86-147741).

[3]   E. J. Violette, Felix Schwering, et al., "Millimeter-Wave Propagation at Street Level in an Urban Environment," IEEE Trans. on Geoscience and Remote Sensing, Vol. 26, No.3, May 1988.

[4]   D. C. Cox, "Time and frequency domain characterizations of multipath propagation at 910 MHz in a suburban mobile-radio environment," Radio Sci., Vol. 7, No. 12., pp. 1069-1077, December 1972.

[5]   D. M. J. Devasirvatham, "Multipath time delay spread in the digital portable radio environment," IEEE Comm. Magazine, Vol. 25, No. 6, June 1987.

[6]   J. G. Proakis, "Digital Communications," (McGraw-Hill 1983), pp. 458-500.

[7]   S. E. Alexander, "Radio propagation within buildings at 900 MHz," Electron. Letters, 1982, 18, pp. 913-914.
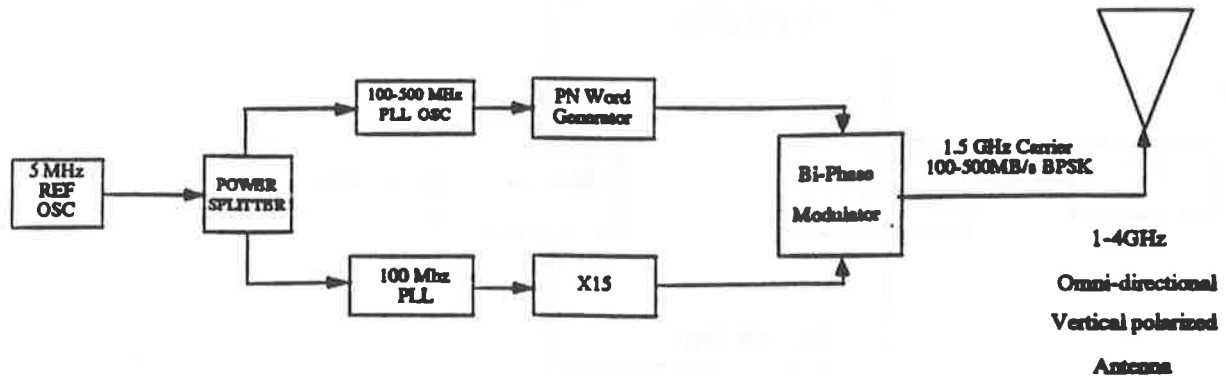
Figure 1. Wideband delay spread system transmitter.
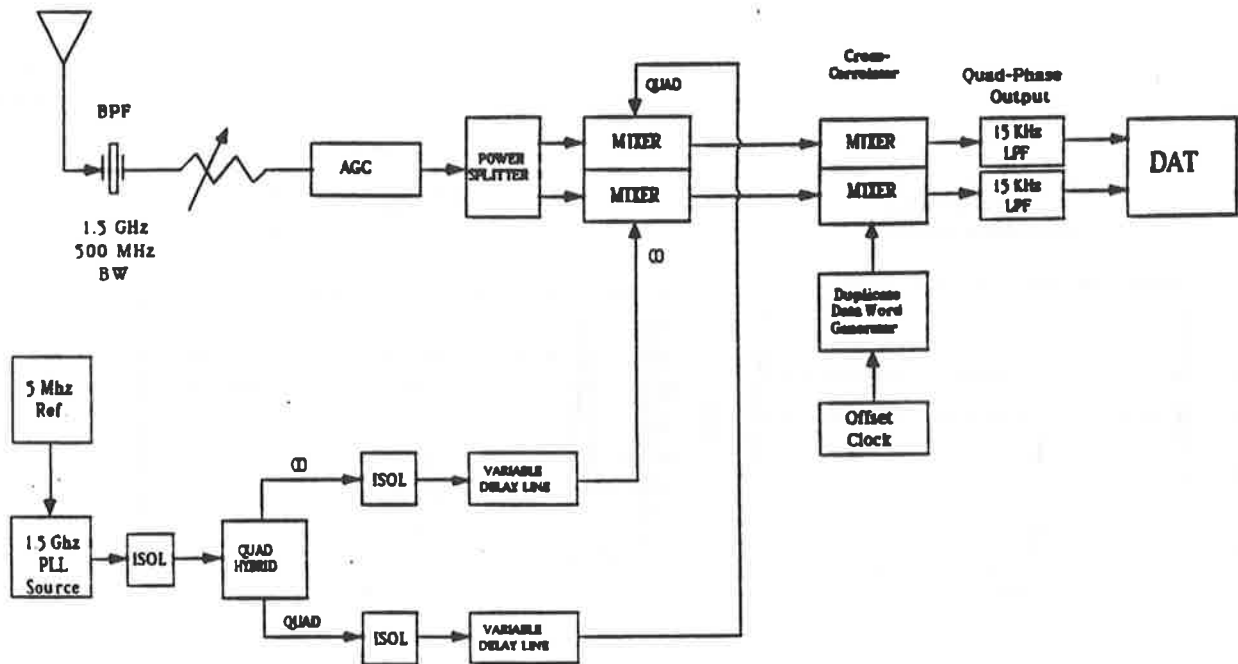
Figure 2. Wideband delay spread system receiver.

1.5m RG55

Td = 8.67ns

```
┌──────────┐      ┌──────────┐        ┌──────────┐      ┌──────────┐
│          │      │  Power   │        │  Power   │      │          │
│    TX    │ ───▶ │ Splitter │        │ Splitter │ ───▶ │    RX    │
│          │      │          │        │          │      │          │
└──────────┘      └──────────┘        └──────────┘      └──────────┘
```

Td = 64.6ns

15.5m
Flexible Waveguide
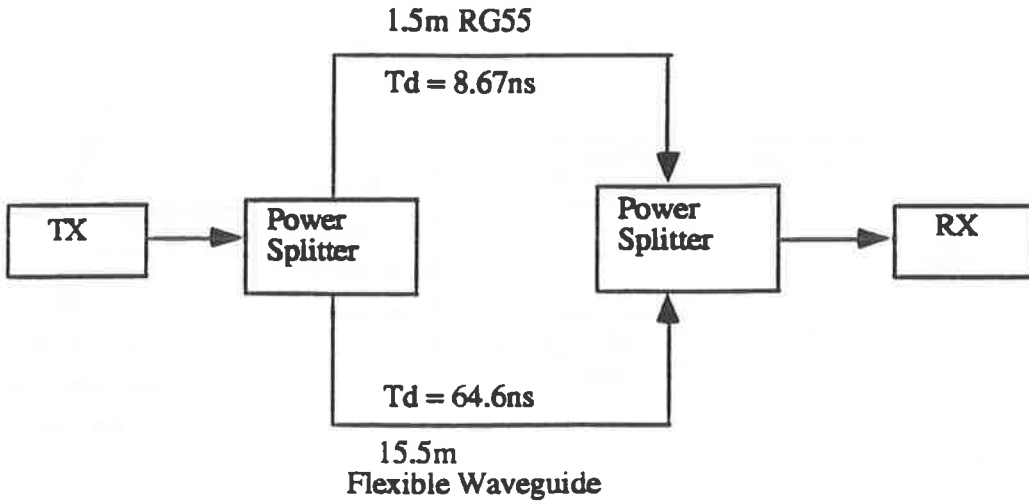
Figure 3.   Calibration test setup.
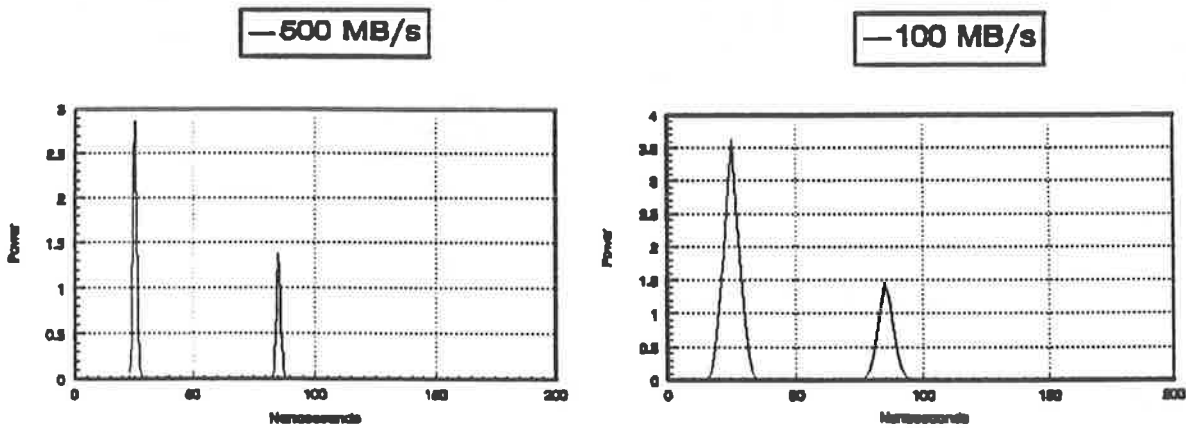
—500 MB/s

—100 MB/s

Figure 4.   Measured calibration data.   Single correlation at 100 and 500 MB/s, 60 ns delay.
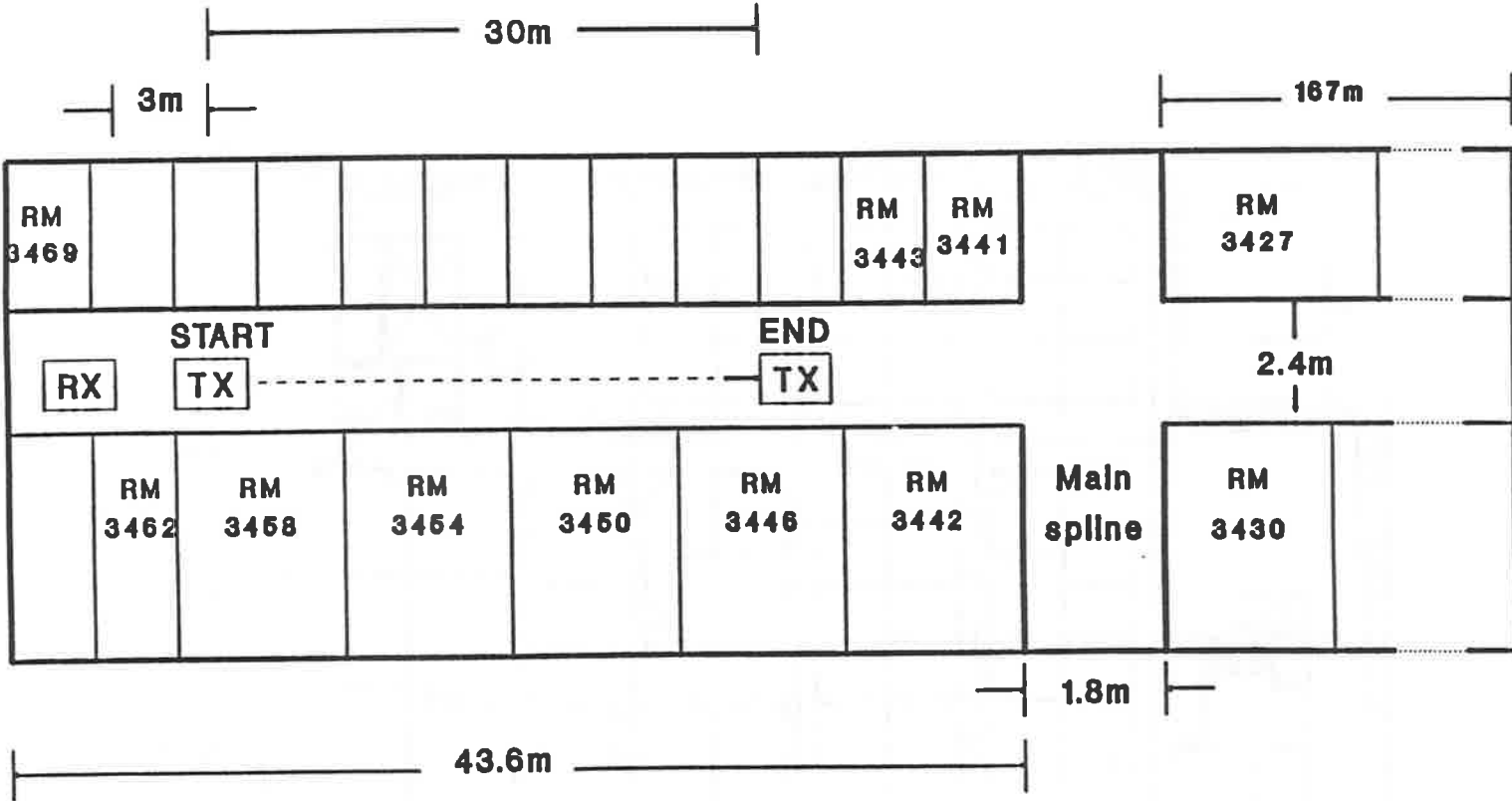
Figure 5. Floor plan and data profile, Wing 4, Radio Building.
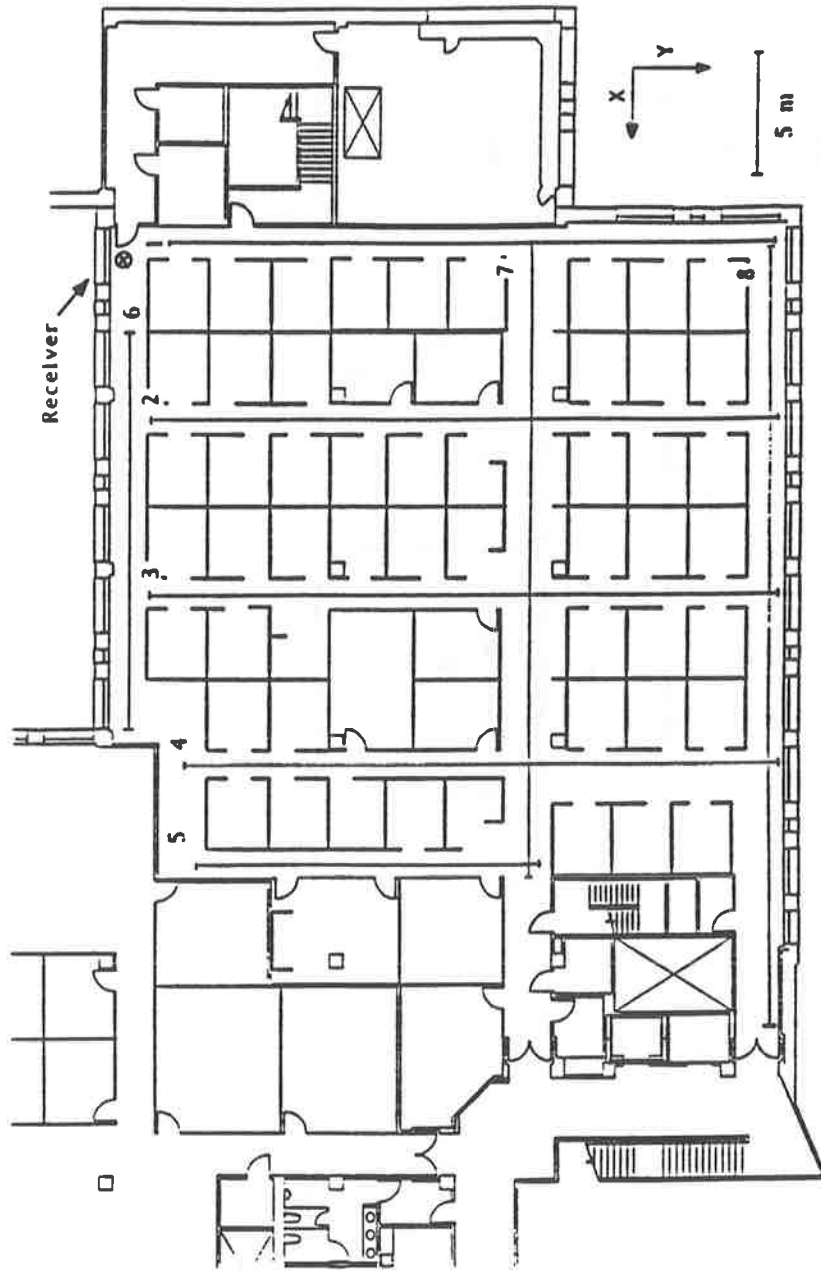
Figure 6. US WEST Room 3200 floor plan with delay spread profile locations and receiver location.
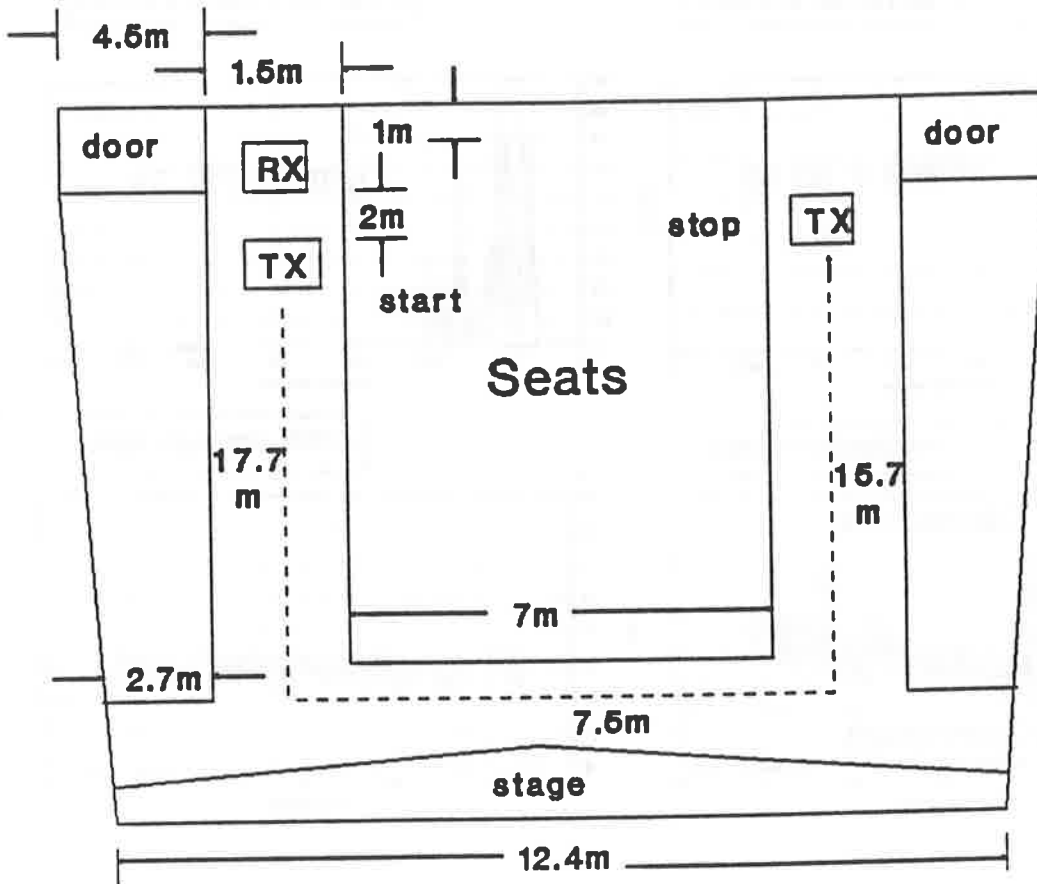
Figure 7. Floor plan, Radio Building auditorium.
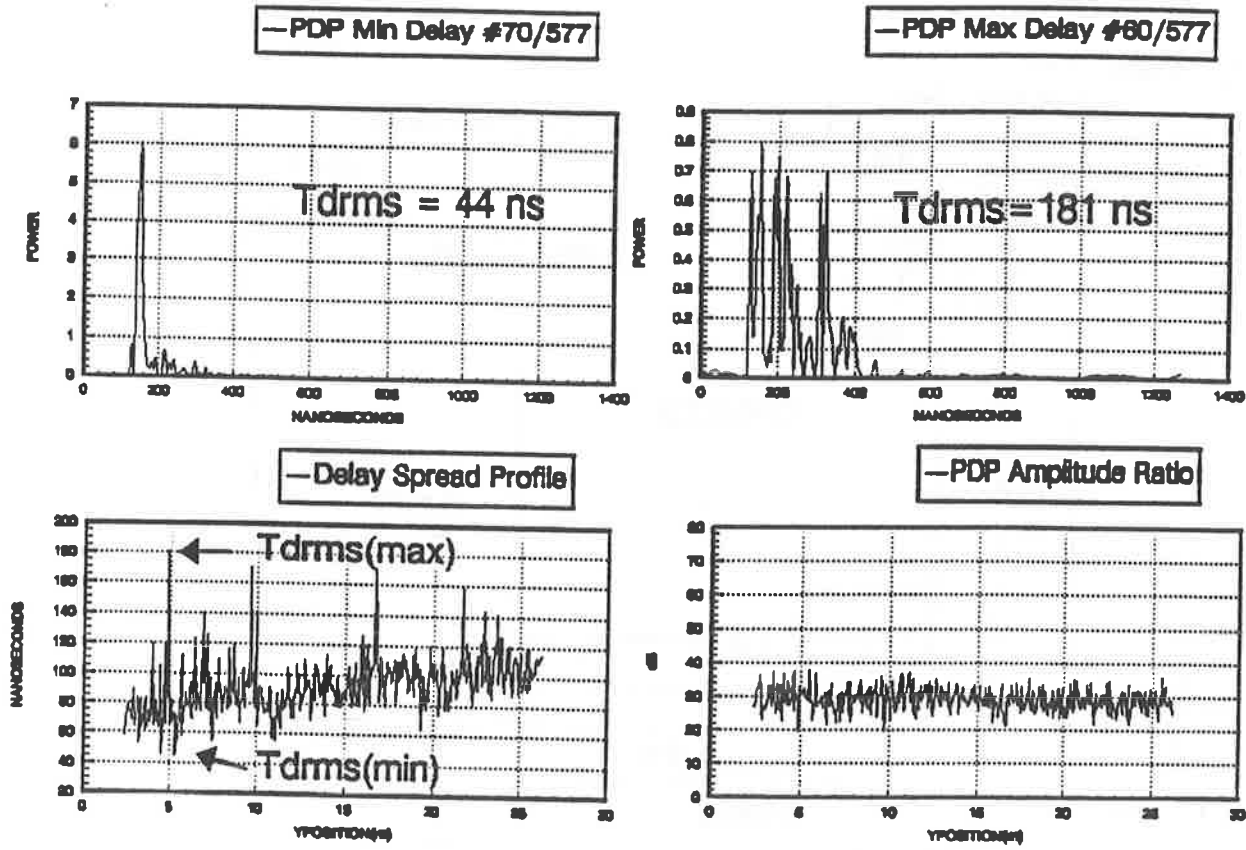
Figure 8. US WEST Profile No. 4, PDP's of max, min delay spreads, delay spread profile, and PDP amplitude ratio.
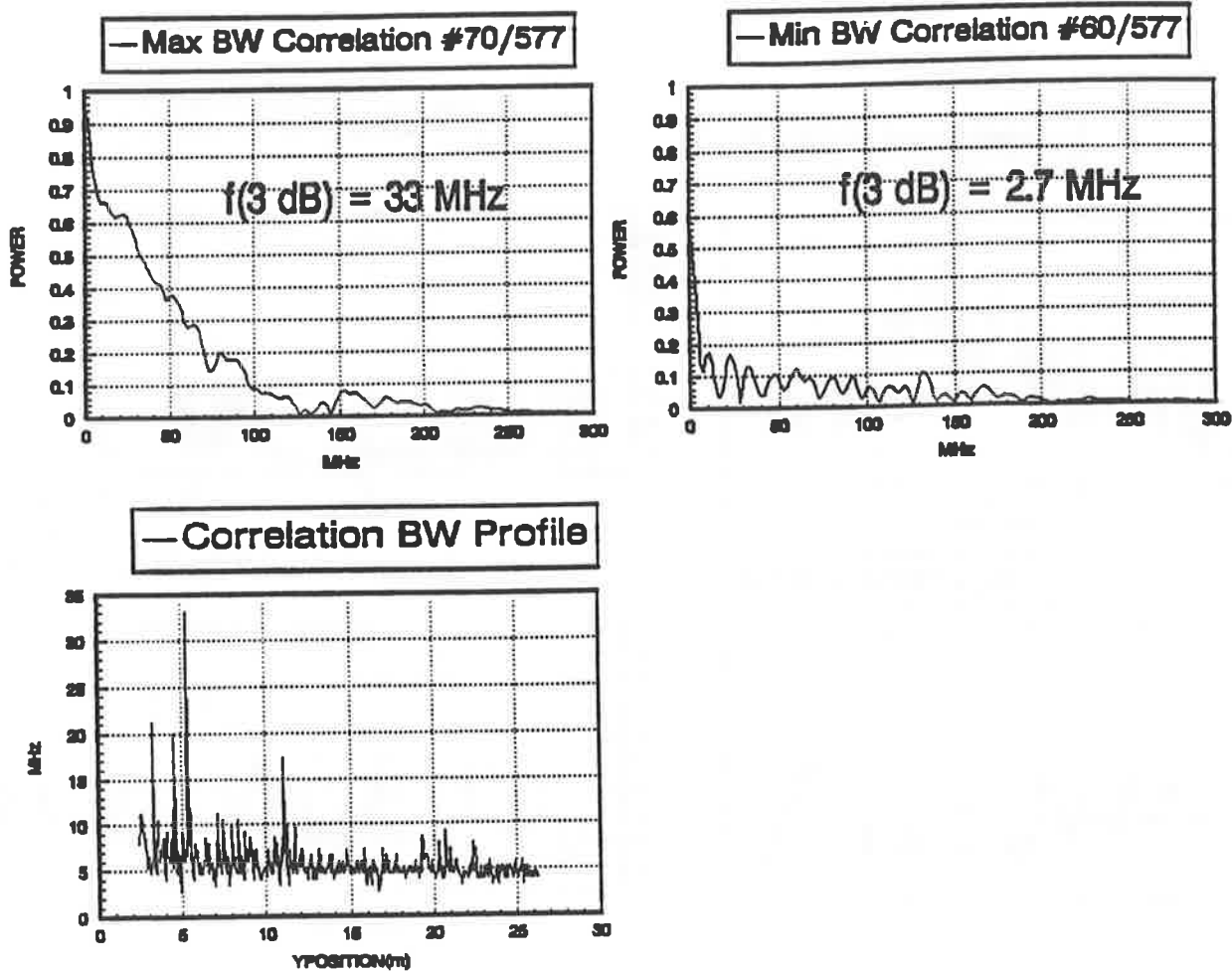
Figure 9. US WEST Profile No. 4, correlation functions for min and max PDP delay spreads, correlation BW profile.
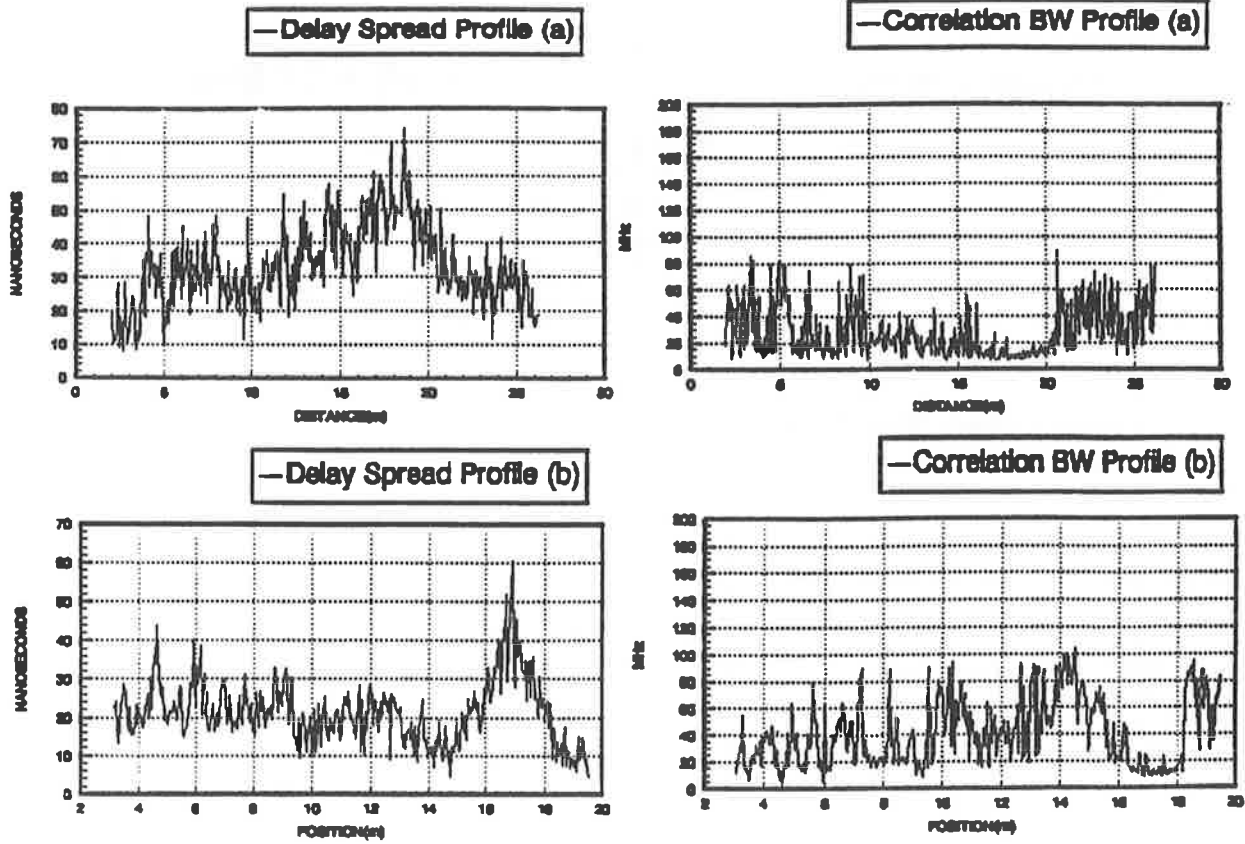
Figure 10. Delay spread and correlation BW profiles. US WEST Rm. 3200 (LOS): Profiles
(a) 1 and (b) 6.
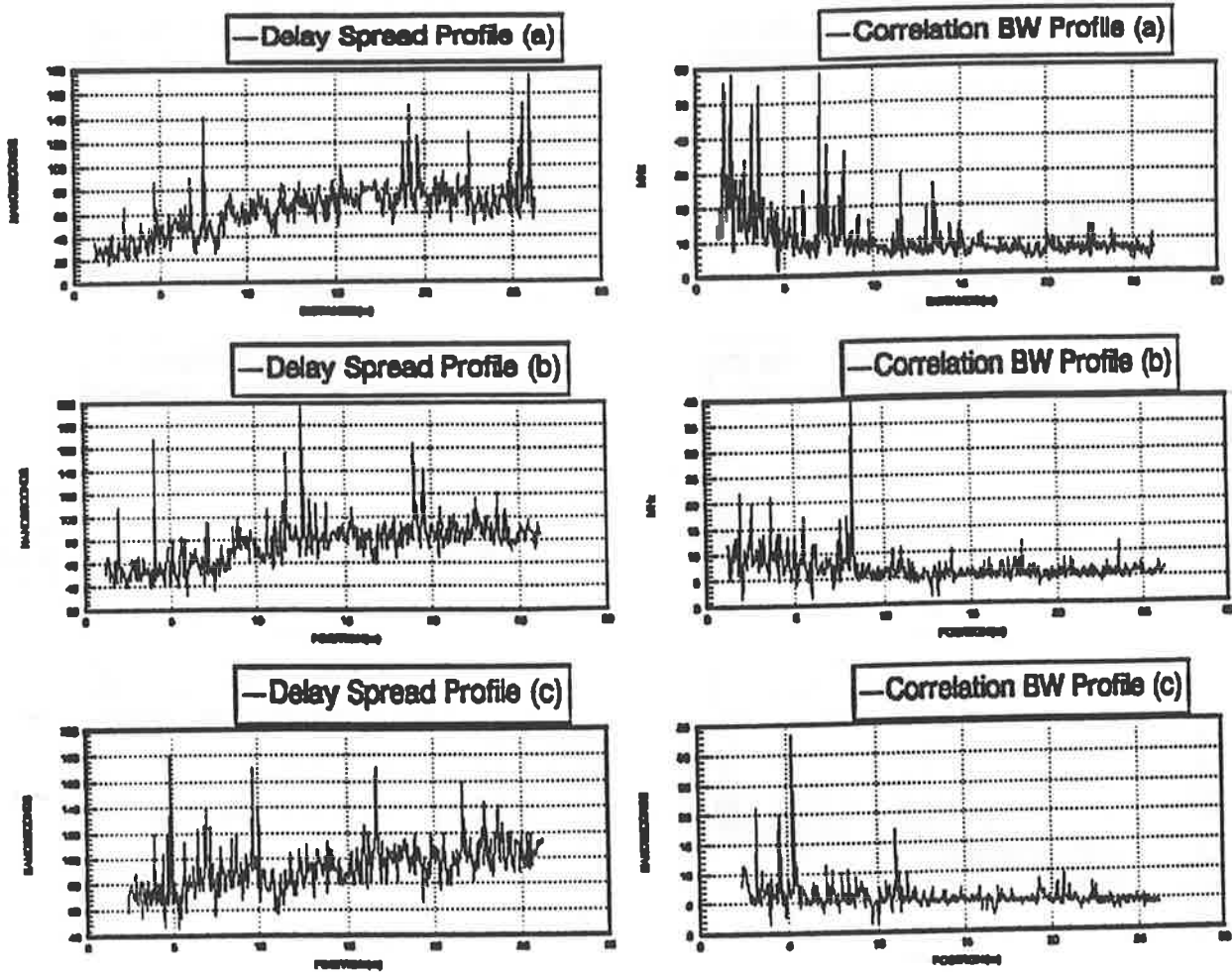
Figure 11. Delay spread and correlation BW profiles. US WEST Rm. 3200 (OLOS):
Profiles (a) 2, (b) 3, and (c) 4.
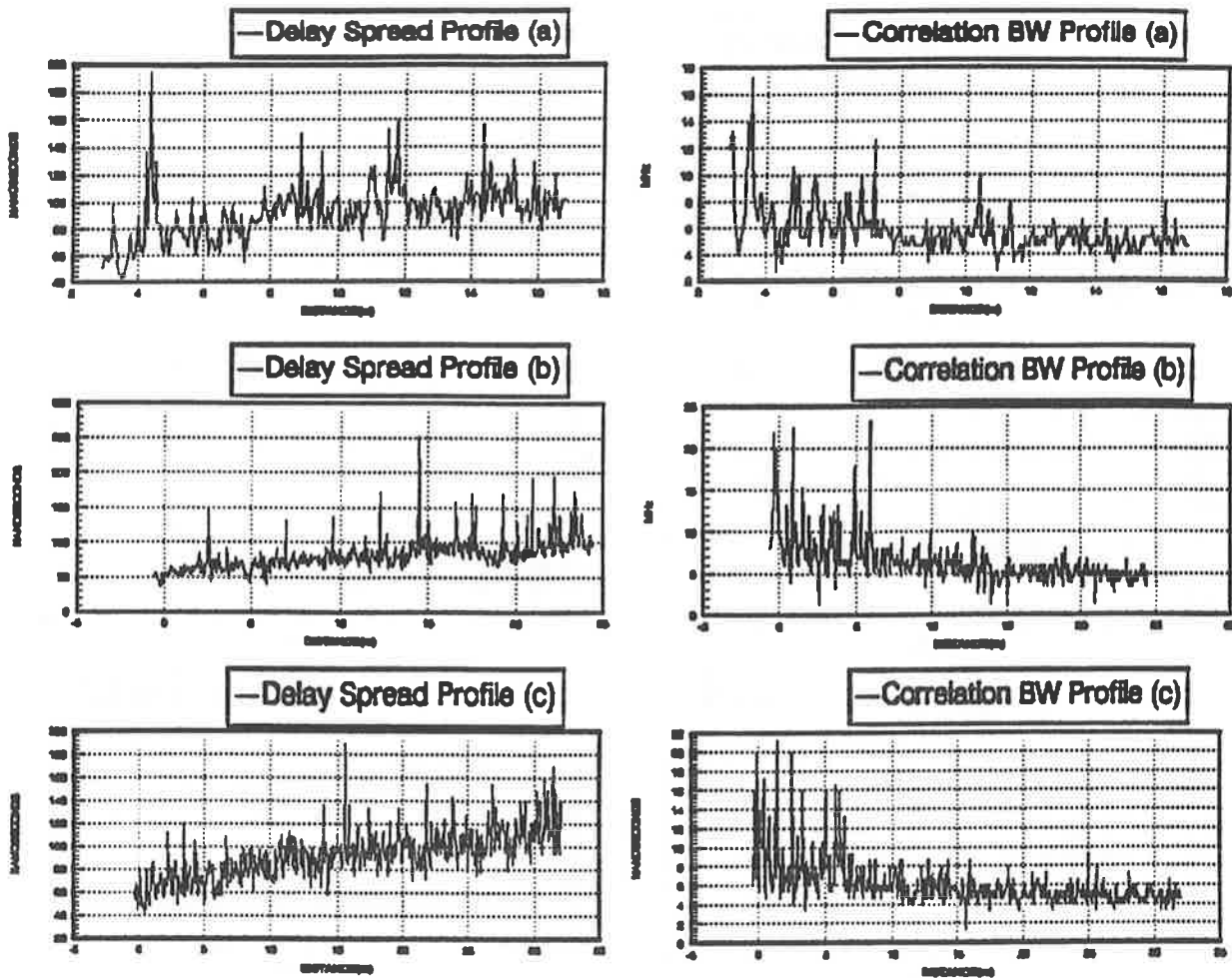
Figure 12. Delay spread and correlation BW profiles. US WEST Rm. 3200 (OLOS):
Profiles (a) 5, (b) 7, and (c) 8.
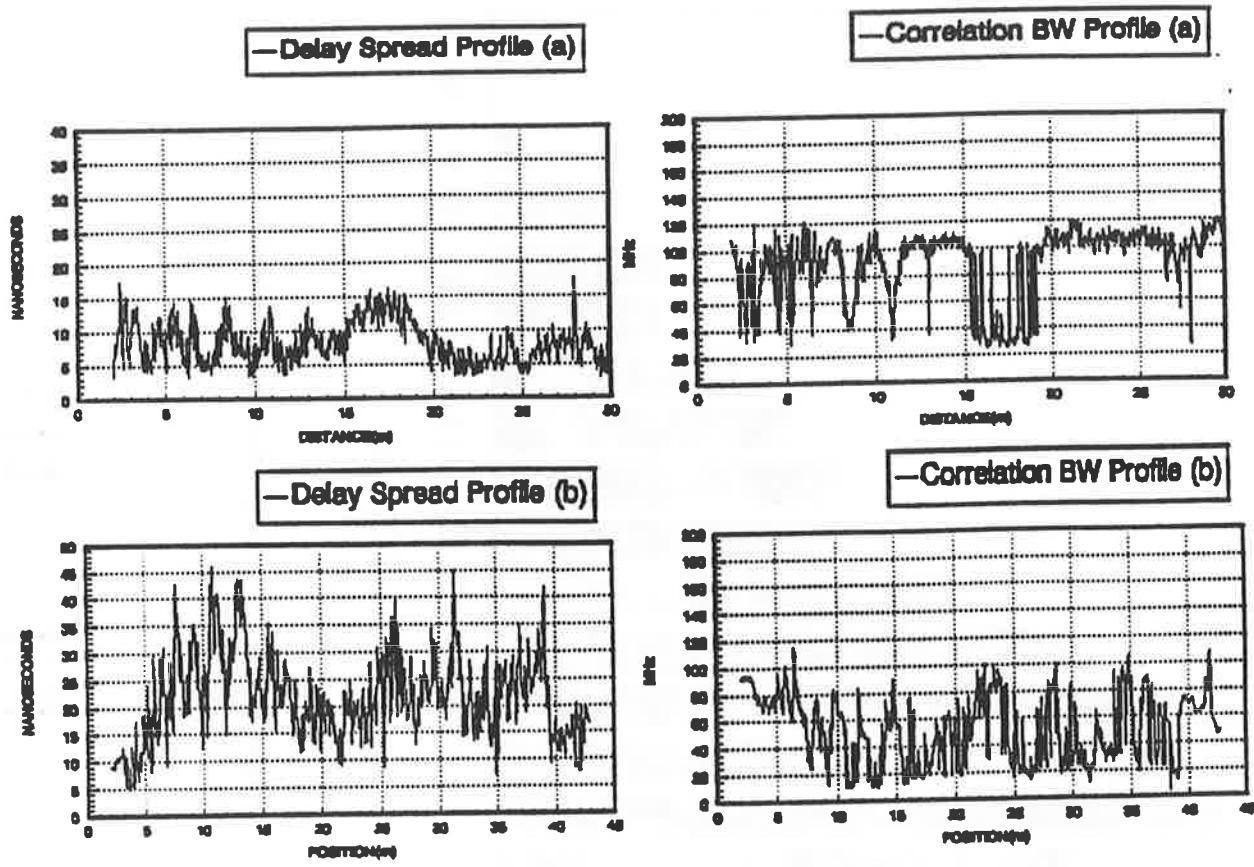
Figure 13. Delay spread and correlation BW profiles. Commerce Radio Building (LOS):
(a) hallway and (b) auditorium.
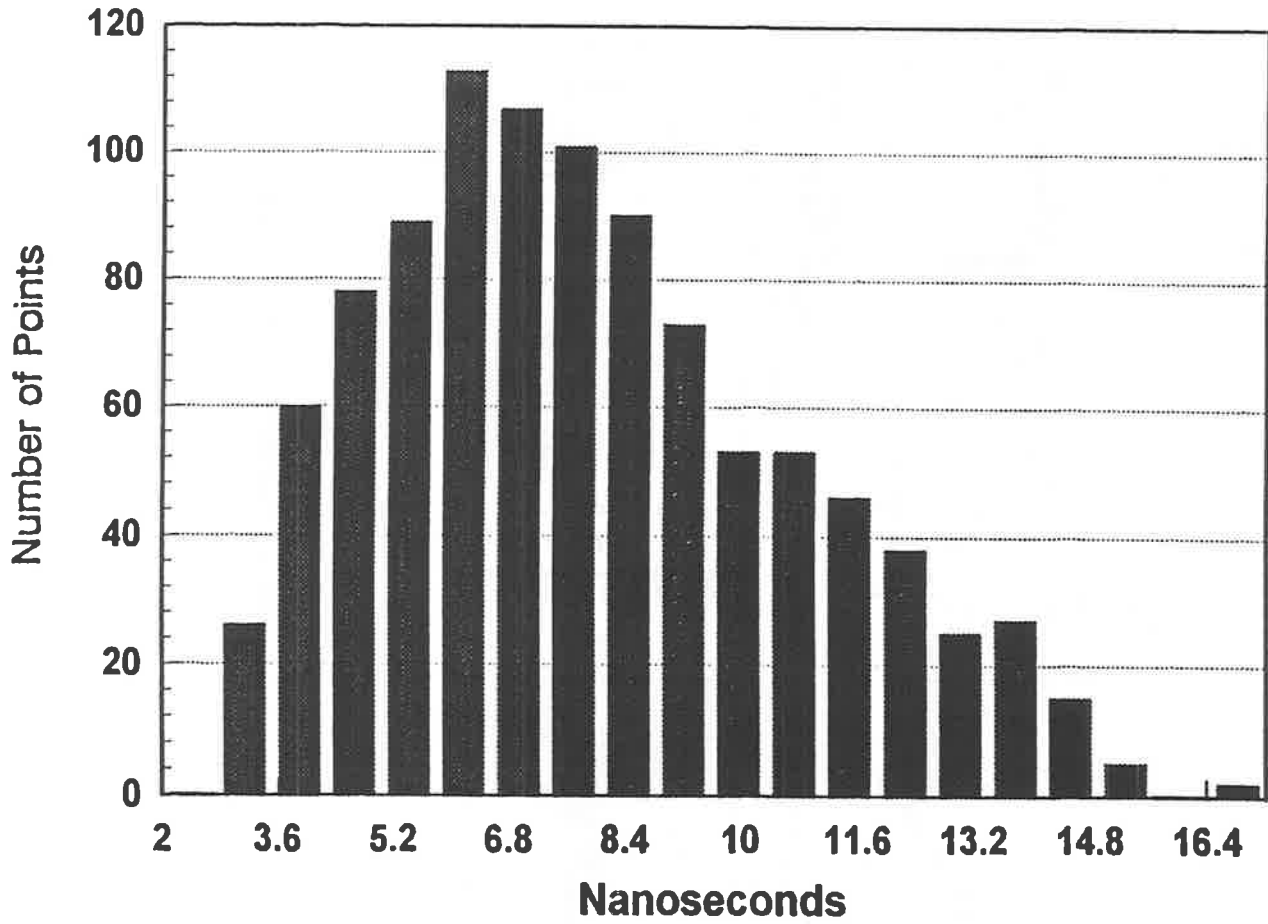
Figure 14a. Histogram of delay spreads, Commerce hallway.
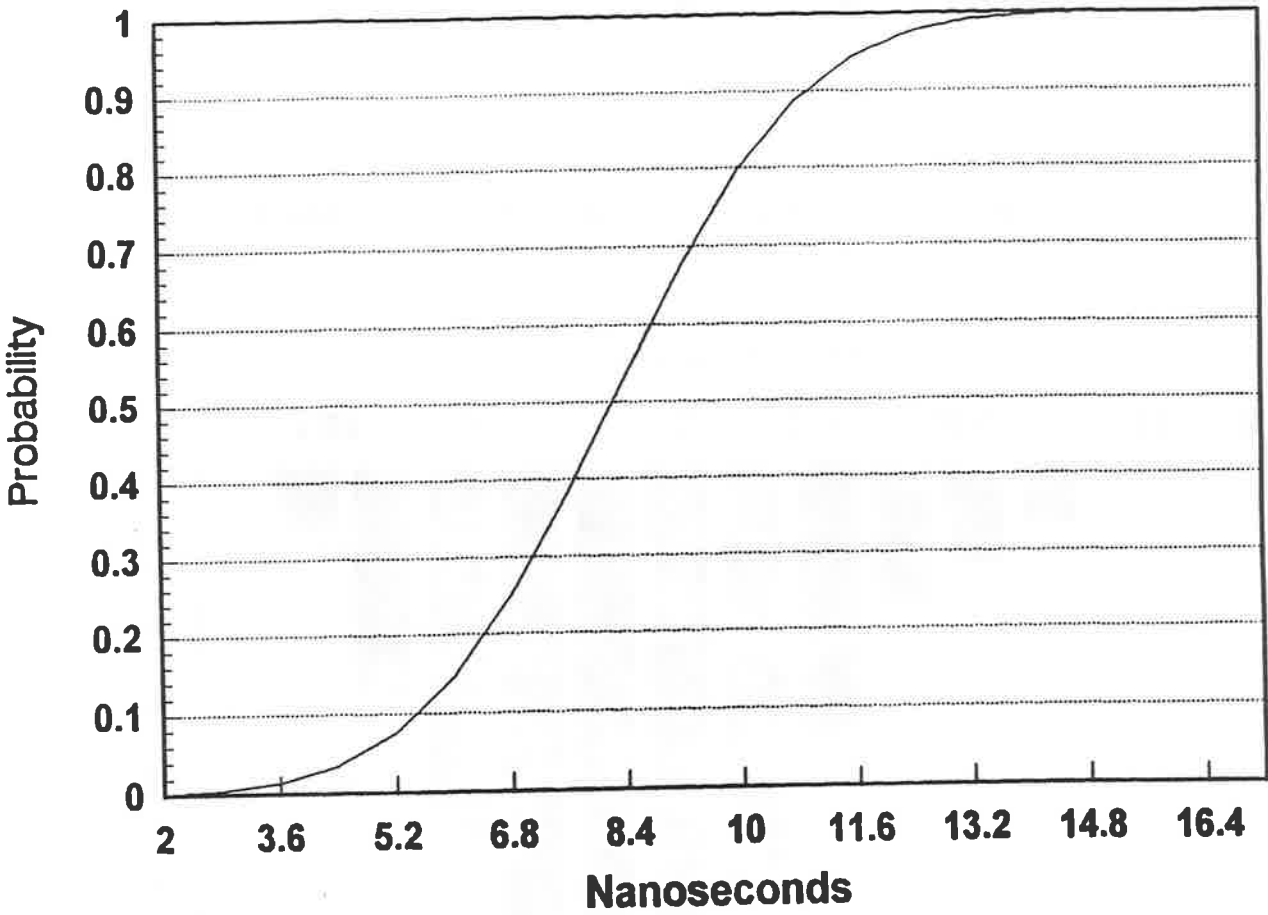
Figure 14b. CDF of delay spreads, Commerce hallway.
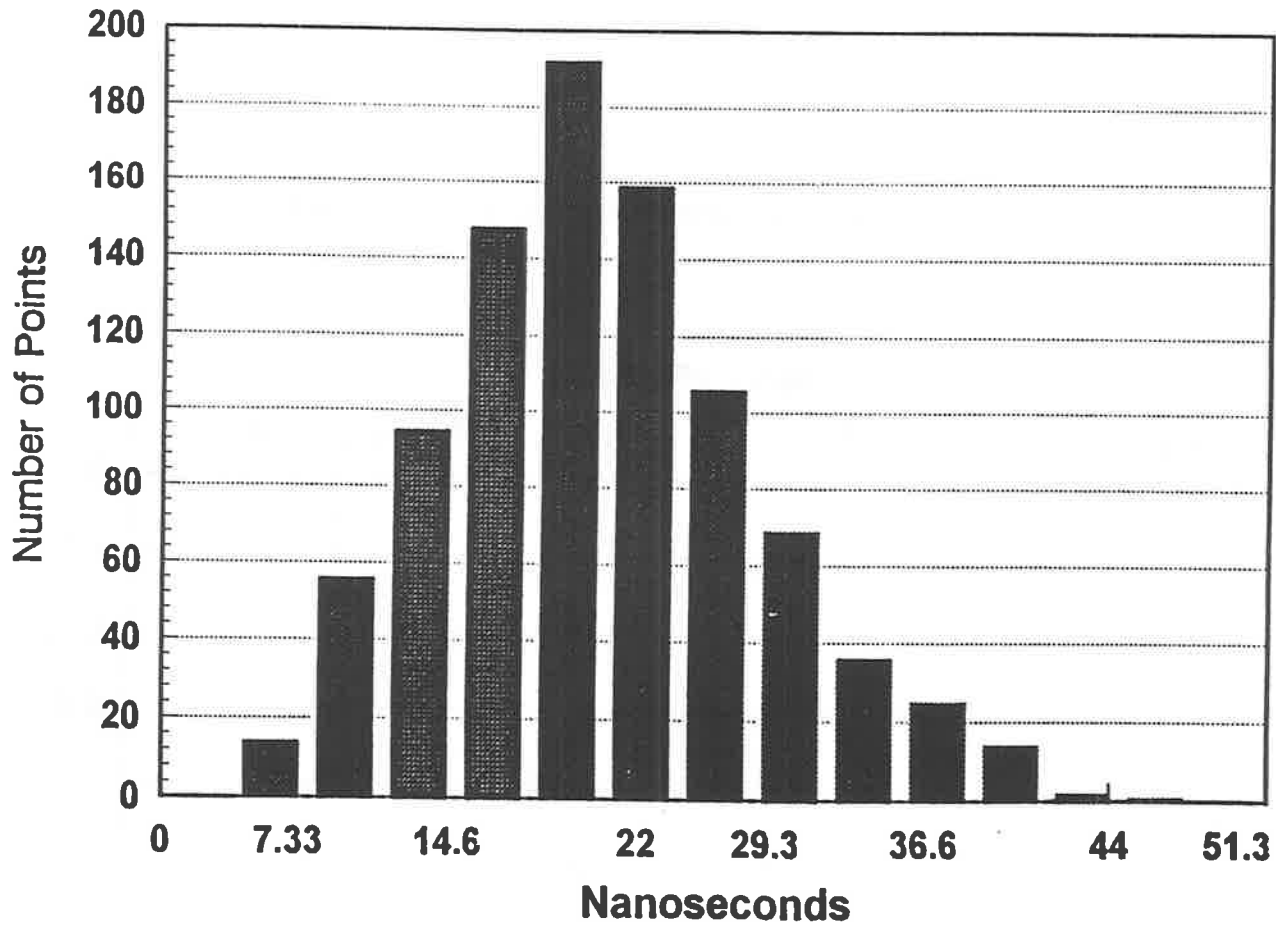
Figure 15a.   Histogram of delay spreads, Commerce auditorium.
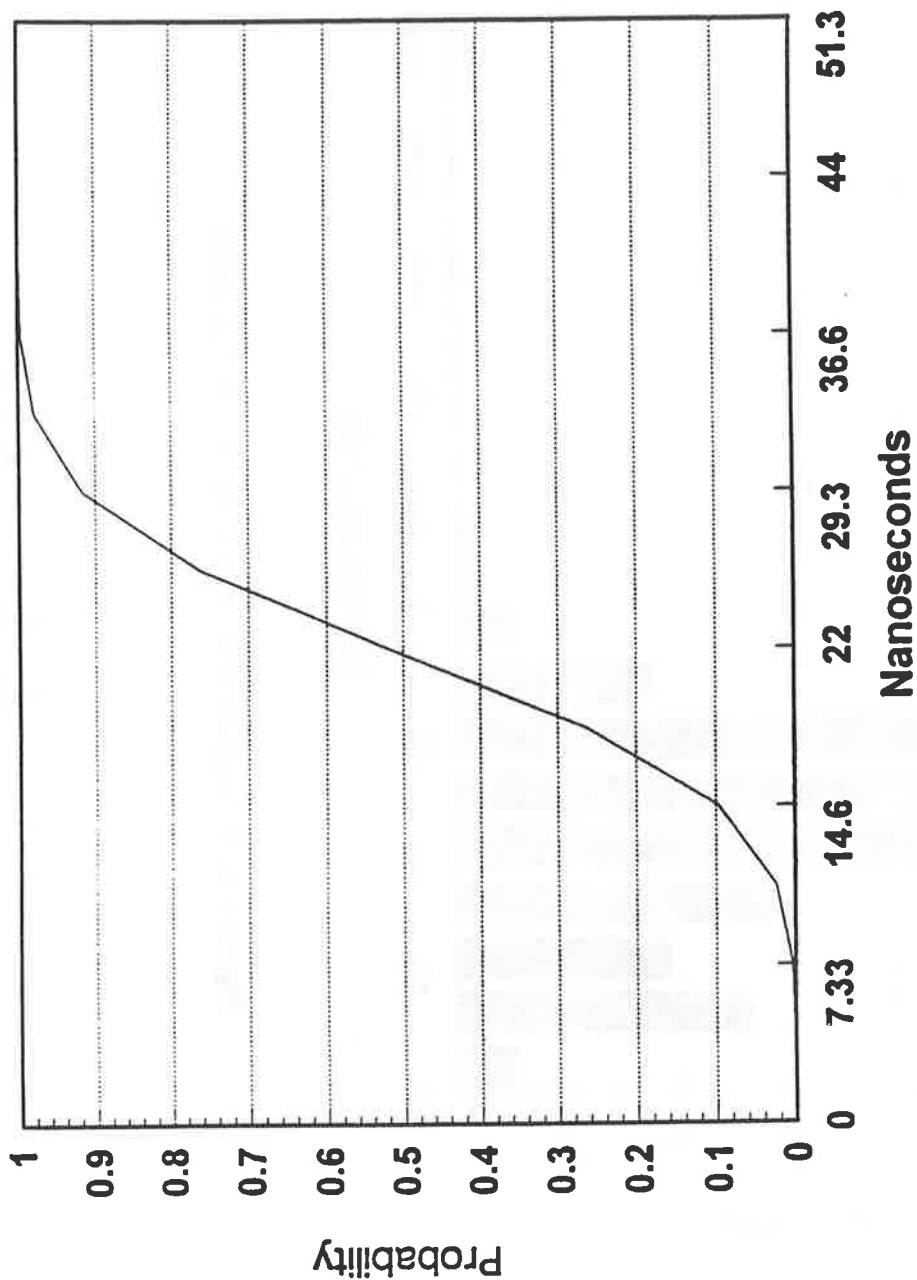
Figure 15b.   CDF of delay spreads, Commerce auditorium.
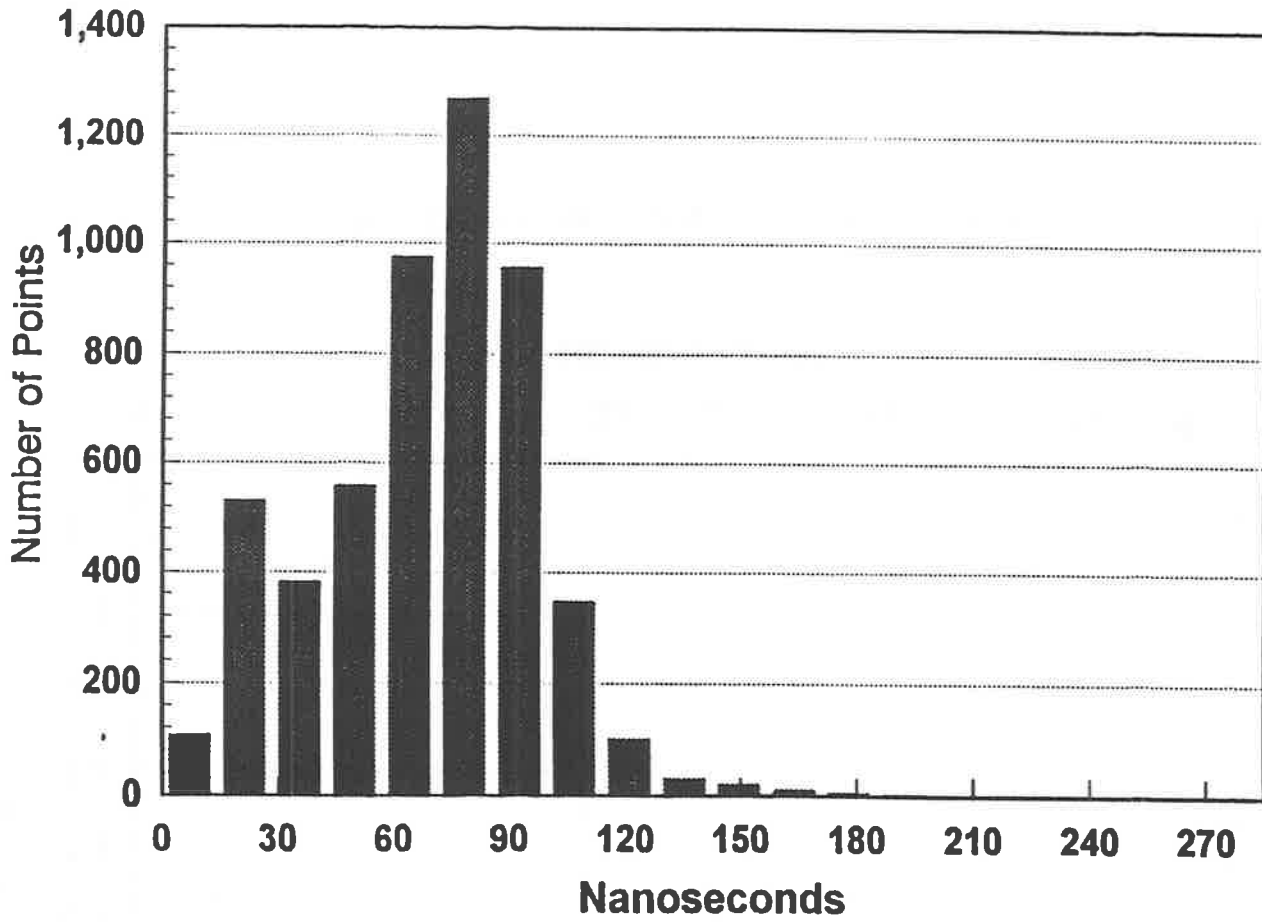
Figure 16a. Histogram of delay spreads, US WEST office.
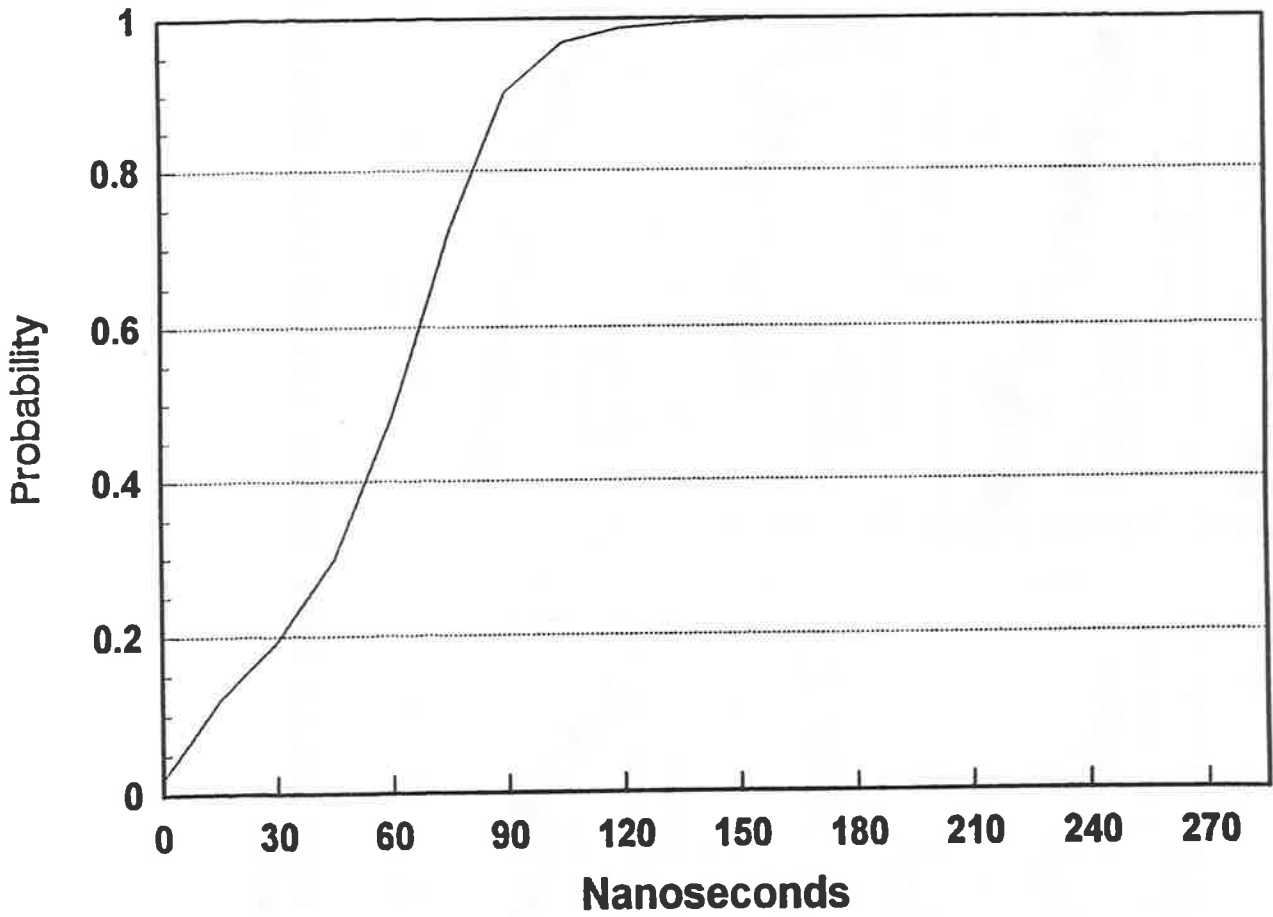
Figure 16b. CFD of delay spreads, US WEST office.
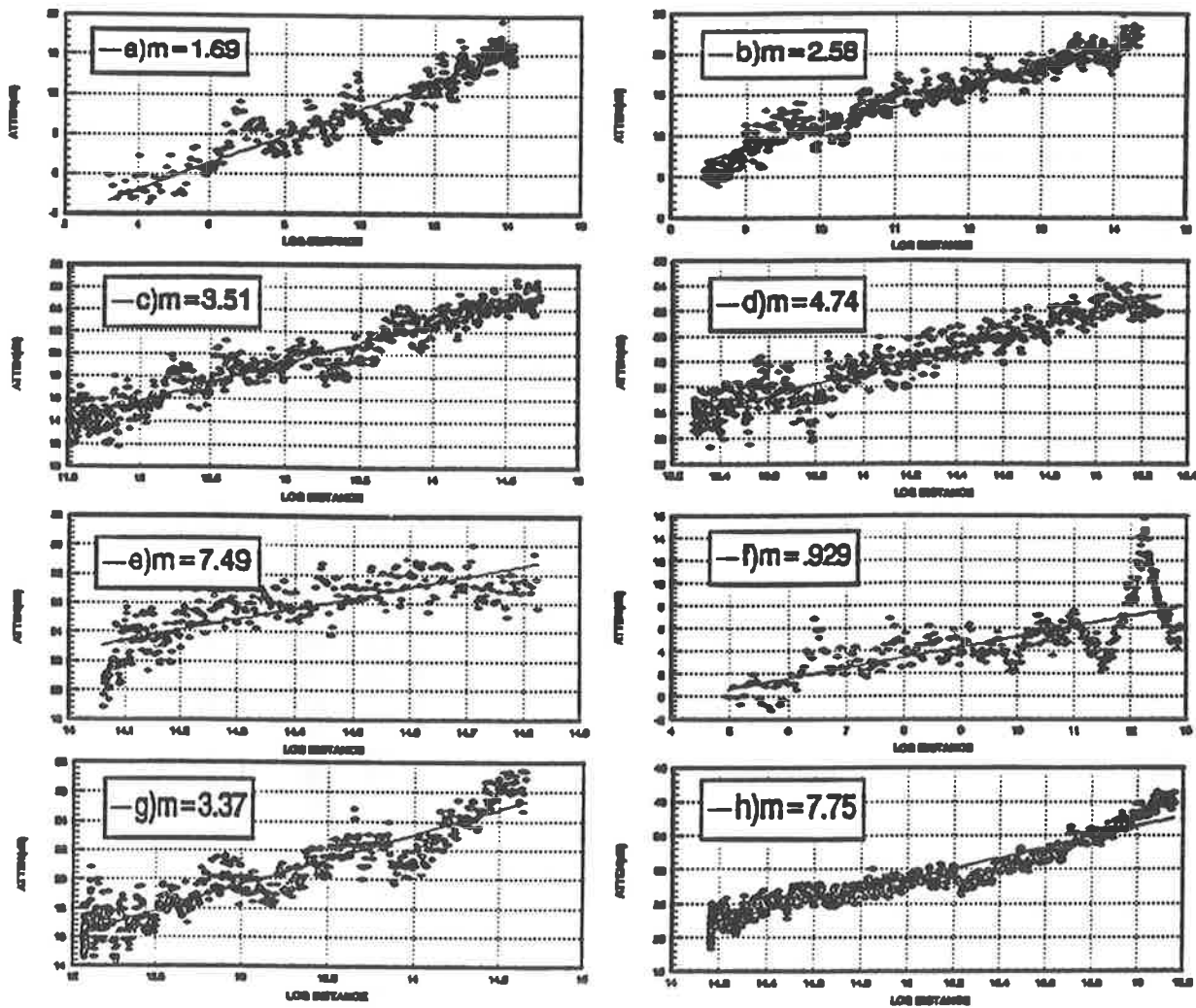
Figure 17. Attenuation scatter plots, US WEST. Profiles: (a) 1, (b) 2, (c) 3, (d) 4, (e) 5, (f) 6, (g) 7, and (h) 8.
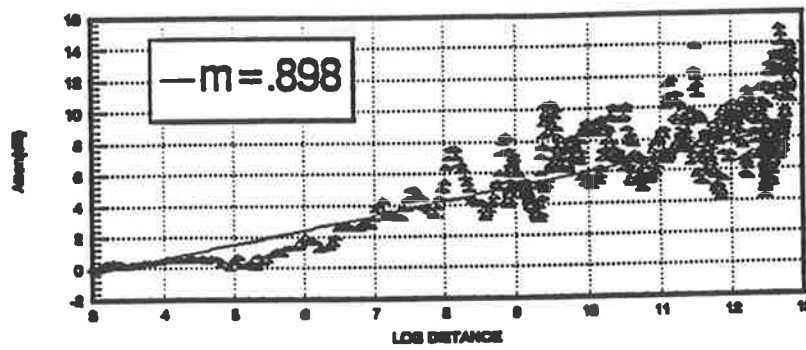
Figure 18. Attenuation scatter plot, auditorium.
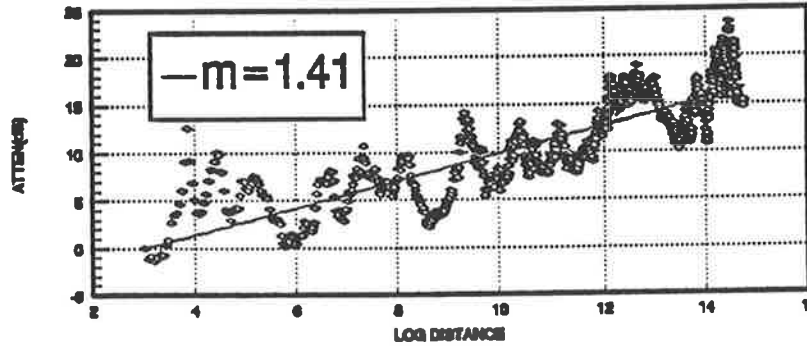
Figure 19. Attenuation scatter plot, hallway.